Hydrologic indicators of hot spots and hot moments of mercury methylation potential along river corridors

Michael Bliss Singer [a,b,*], Lee R. Harrison [b,c], Patrick M. Donovan [d], Joel D. Blum [d], Mark Marvin-DiPasquale [e]

[a] Department of Earth & Environmental Sciences, University of St Andrews, St Andrews, UK
[b] Earth Research Institute, University of California Santa Barbara, Santa Barbara, CA, USA
[c] NOAA Fisheries, Santa Cruz, CA, USA
[d] Department of Earth & Environmental Sciences, University of Michigan, Ann Arbor, MI, USA
[e] National Research Program, Water Resources Division, US Geological Survey, Menlo Park, CA, USA

HIGHLIGHTS

- Flood magnitude, frequency, and duration are relevant to mercury methylation potential (MPP).
- Methylmercury is present in aquatic biota at various trophic levels.
- We estimate MPP from surface sediment by floodplain inundation, 1967–2013.
- Longer floods in the historical record are tied to higher MPP than shorter ones.
- The legacy of 19th Century hydraulic gold mining in CA is one of ongoing toxicity to food webs.

GRAPHICAL ABSTRACT

ABSTRACT

The biogeochemical cycling of metals and other contaminants in river-floodplain corridors is controlled by microbial activity responding to dynamic redox conditions. Riverine flooding thus has the potential to affect speciation of redox-sensitive metals such as mercury (Hg). Therefore, inundation history over a period of decades potentially holds information on past production of bioavailable Hg. We investigate this within a Northern California river system with a legacy of landscape-scale 19th century hydraulic gold mining. We combine hydraulic modeling, Hg measurements in sediment and biota, and first-order calculations of mercury transformation to assess the potential role of river floodplains in producing monomethylmercury (MMHg), a neurotoxin which accumulates in local and migratory food webs. We identify frequently inundated floodplain areas, as well as floodplain areas inundated for long periods. We quantify the probability of MMHg production potential (MPP) associated with hydrology in each sector of the river system as a function of the spatial patterns of overbank inundation and drainage, which affect long-term redox history of contaminated sediments. Our findings identify river floodplains as periodic, temporary, yet potentially important, loci of biogeochemical transformation in which contaminants may undergo change during limited periods of the hydrologic record. We suggest that inundation is an important driver of MPP in river corridors and that the entire flow history must be analyzed retrospectively in terms of

* Corresponding author.
E-mail address: bliss@eri.ucsb.edu (M.B. Singer).

inundation magnitude and frequency in order to accurately assess biogeochemical risks, rather than merely highlighting the largest floods or low-flow periods. MMHg bioaccumulation within the aquatic food web in this system may pose a major risk to humans and waterfowl that eat migratory salmonids, which are being encouraged to come up these rivers to spawn. There is a long-term pattern of MPP under the current flow regime that is likely to be accentuated by increasingly common large floods with extended duration.

1. Introduction

Mercury (Hg) contamination of food webs is a global problem with severe consequences for ecosystem and human health (Cristol et al., 2008; Mergler et al., 2007). Anthropogenic sources of inorganic divalent Hg (Hg^{2+}), hereafter referred to as iHg, enter the environment primarily through atmospheric emissions (and deposition) or through point source releases from historical mining. In the environment, iHg can be biogeochemically processed into monomethylmercury (MMHg) that is toxic to biota and becomes bioconcentrated and biomagnified in food webs. Currently there is limited understanding of the production of MMHg along river corridors due to the complex interactions between inundation history and net transport/deposition of contaminated sediment.

Flooding affects redox history and thus supports the activity of bacteria that are responsible for converting iHg to its more toxic, bioavailable form, MMHg. This conversion is based on biologically mediated reactions that are thought to occur in locations and time periods of low oxygen at the sediment-water interface (Beutel et al., 2008). There is currently a well-documented understanding of MMHg production by anaerobic bacteria in laboratory settings, (e.g., Compeau and Bartha, 1985; Gilmour et al., 1992; Kerin et al., 2006), but there are major outstanding uncertainties regarding loci, timing and rates of Hg (II) methylation in natural fluvial systems, especially at the landscape scale. In river basins affected by high levels of iHg contamination, for example due to historical mining, there may be great variability in spatial patterns of total Hg concentrations (THg) in channel boundary sediment (Miller et al., 1999; Miller, 1997; Pizzuto, 2012; Singer et al., 2013), yet the spatiotemporal variability of redox might be a more dominant control over microbial activity. There is limited systematic understanding of where and when MMHg is produced in river corridors. This could, in part, be due to spatial or temporal biases in prior investigations emphasizing particular river reaches or sampling over a limited timeframe, which masks the impact of important hydrologic events (Balogh et al., 2006; Blum et al., 2001; Domagalski, 1998; Domagalski, 2001; Marvin-DiPasquale et al., 2009b). It could also be due to a lack of attention to less obvious locations in the watershed, such as river floodplains, that exhibit suboxic conditions only temporarily, associated with large inundation events or within hyporheic flow (Briggs et al., 2015; Hinkle et al., 2014). Thus, the zone of potential Hg methylation may expand and contract vertically and laterally with flood cycles (Creswell et al., 2008).

It is conventionally assumed that MMHg production mainly occurs in wetland environments or in lakes (Benoit et al., 2003; Coleman Wasik et al., 2015; Grigal, 2002; Krabbenhoft et al., 1995; St. Louis et al., 1994), where oxygen levels are relatively low such that anaerobic sulfate-reducing bacteria (SRB) and iron reducing bacteria (FeRB) primarily responsible for Hg methylation can thrive (Gilmour et al., 1992; Gilmour et al., 2013). However, there are limits to this view of Hg methylation. The following have been shown in prior work. 1) The percentage of wetland area within a basin may be a poor predictor of MMHg concentrations in certain river basins (Tsui et al., 2009a), suggesting the importance of other Hg methylation zones along some rivers. 2) There is, in some basins (but see Grigal, 2002), a tenuous relationship between lowland wetland area and MMHg in local pore water within sediments, suggesting the prevalence of upstream MMHg production in some lotic settings (Marvin-DiPasquale et al., 2009b). 3) High MMHg concentrations have been found in non-migratory algae, benthic macrointvertebrates, and fish in parts of river basins well upstream of lowland floodplains/wetlands (Buckman et al., 2015; Donovan et al., In Review; Donovan et al., 2016; Tsui et al., 2009a). 4) Cycles of wetting and drying have been shown to increase Hg concentrations within fish in lake systems (Sorensen et al., 2005), suggesting that non-permanent wetland areas may be important sites for conversion of iHg to MMHg. 5) MMHg production has been shown to be driven by flood events that infrequently inundate large areas adjacent to the channels (Balogh et al., 2006).

Thus, it is possible that upland riverine environments play an important role in MMHg production, which has been largely overlooked. Clearly, there are relevant factors affecting mercury methylation on the landscape scale that have not been well documented or quantified. The extension of streamflow from river channels into floodplains is understood to influence oxygen availability and affect biogeochemical processing of phosphorus, nitrogen, and sulfur (Baldwin and Mitchell, 2000), so it follows that the so-called flood pulse (Junk et al., 1989; Tockner et al., 2000) should also play a role in Hg biogeochemistry. In fact, recent research has suggested that the hyporheic zone along stream channels may control MMHg production (Bradley et al., 2012; Hinkle et al., 2014), but there is very limited research on this topic. Spatial and temporal variability in streamflow directly affects the extent, timing, and persistence of inundated surfaces along a river. Sequences of flood events generate complex inundation histories banks, terraces, and floodplains that have the potential to alter local redox conditions and thereby affect the microbial conversion of iHg to MMHg (Benoit et al., 1999; Benoit et al., 1998; Gilmour et al., 1992; Schaefer and Morel, 2009; Wallschlager et al., 1998), potentially increasing or decreasing the likelihood of MMHg introduction into aquatic food webs. In summary, the infrequent extension of flooding from channels into floodplains dramatically reduces oxygen supplies within sediment as pore spaces become filled with water rather than air (typically decreasing pore oxygen content by >3 orders of magnitude). Subsequently, oxygen becomes limited due to lack of replenishment from the atmosphere, thus stimulating anaerobic bacterial processes (Briggs et al., 2015). Therefore, the frequency and duration of floods and their spatial extent in the landscape may be critical to riverine Hg biogeochemistry.

This paper addresses the spatial and temporal dimensions of MMHg production potential at the landscape scale within a large, Hg-contaminated watershed. We use hydraulic modeling over a decadal timeframe to infer the frequency and duration of land surface inundation across this watershed, which we interpret as a proxy for temporary suboxic conditions conducive to MMHg production potential (Podar et al., 2015). We aim to infer the past history of mercury dynamics by identifying locations in a large drainage basin that may be considered 'hot spots' of MMHg production due to frequent inundation, as well as particular flood events that may be considered 'hot moments' of MMHg production due to prolonged inundation. We note that these definitions of 'hot spots' and 'hot moments' differ from those used in prior research on biogeochemical transformation (McClain et al., 2003), where the focus was on accelerated rates of biogeochemical changes. However, we believe these adapted terms represent reasonable extensions which highlight the specific role of variable hydrology in affecting redox over a large area. We set out to answer these questions: 1) What are the spatial and temporal patterns of inundation in the river-floodplain corridor? 2) How does the history of inundation

relate to MMHg production potential and contamination of riverine food webs?

2. Study area and past research

We conducted this work in the Sacramento Valley, California, which is still evolving topographically (Singer et al., 2013) and biogeochemically (Donovan et al., 2013; Gehrke et al., 2011a,2011b; Marvin-DiPasquale and Agee, 2003; Marvin-DiPasquale et al., 2014) in response to 19th century hydraulic gold mining in the Sierra Nevada foothills. Mining produced widespread landscape-scale contamination of waterways, floodplains, benthic sediment, and aquatic biota within the watershed (Bouse et al., 2010; Conaway et al., 2007; Domagalski, 1998; Domagalski, 2001; Donovan et al., 2016; Eagles-Smith et al., 2009; Greenfield and Jahn, 2010; Greenfield et al., 2013; Henery et al., 2010; Singer et al., 2013; Springborn et al., 2011; van Geen and Luoma, 1999) and recent research using Hg isotopes has suggested a link between biotic contamination and co-located sediment (Donovan et al., 2016; Gehrke et al., 2011a). Detailed datasets are available for this study area including iHg, high-resolution digital elevation models-DEMs and daily flow history over many decades, thus providing an excellent opportunity to investigate relationships between flow history and potential contamination of the aquatic ecosystem.

The study area comprises the Lower Yuba/Feather River system along ~70 km of river corridor (Fig. 1). We document river and flood-plain inundation along the main Yuba and Feather River channels from the Yuba Gold Fields in the middle course of the Lower Yuba into the Feather River at its confluence within the twin cities of Marysville and Yuba City, and through the Feather to its confluence with Sutter Bypass, a lowland floodway along the Sacramento River within California's Central Valley. The study area has been identified as a long zone of Hg contamination produced by sediment transport contemporaneous with 19th century hydraulic gold mining (Gilbert, 1917; Hunerlach et al., 1999), augmented by episodic delivery of reworked mining

sediment from upstream to downstream (Higson and Singer, 2015; Kilham, 2009; Kilham et al., 2012; Singer et al., 2013). Recent work documented total Hg concentrations (THg) at various topographic positions and within chemostratigraphy along all of these river courses and within their floodplains (Singer et al., 2013).

Our prior work demonstrated that: 1) THg in sediment is well above background concentrations in most of this region; 2) THg decreases due to dilution with uncontaminated sediment in transit from upstream to downstream; and 3) THg varies with vertical position within stratigraphy as a function of the timing of deposition and subsequent reworking by fluvial processes (Ghoshal et al., 2010; Singer et al., 2013). In recent work, our team documented through MMHg, THg, and Hg isotope measurements that sediment-bound Hg along the Yuba-Feather system is a likely source of iHg and MMHg to aquatic organisms within these streams (Donovan et al., 2016). In other words, we suggested that Hg contamination of the riverine food web in this area is likely associated with the legacy of historic gold mining, rather than with an atmospheric source or one that is transported in the water column from upstream (e.g., reservoirs). This means that the local environment in which Hg-laden sediment deposits reside are potentially important sites for iHg methylation leading to MMHg bioaccumulation and trophic transfer in local food webs. Thus, it is important to determine whether the flow regime of these rivers may contribute over decadal timescales to food web contamination by temporarily altering redox conditions, thereby generating a local source of MMHg.

The flow regime in this river system is typical of a Mediterranean climate (wet winters and dry summers) with episodic, punctuated by large, valley-filling floods (Fig. 2) that occur approximately once a decade (Higson and Singer, 2015; Singer et al., 2013), despite the presence of upstream dams (Singer, 2007), with long relatively quiescent periods in between. Rivers draining the Sierra Nevada Mountains - especially the Yuba River - are of great interest to river restoration practitioners and scientists looking to recreate/expand the current spawning habitat for migratory salmon within the heavily impacted Sacramento Valley
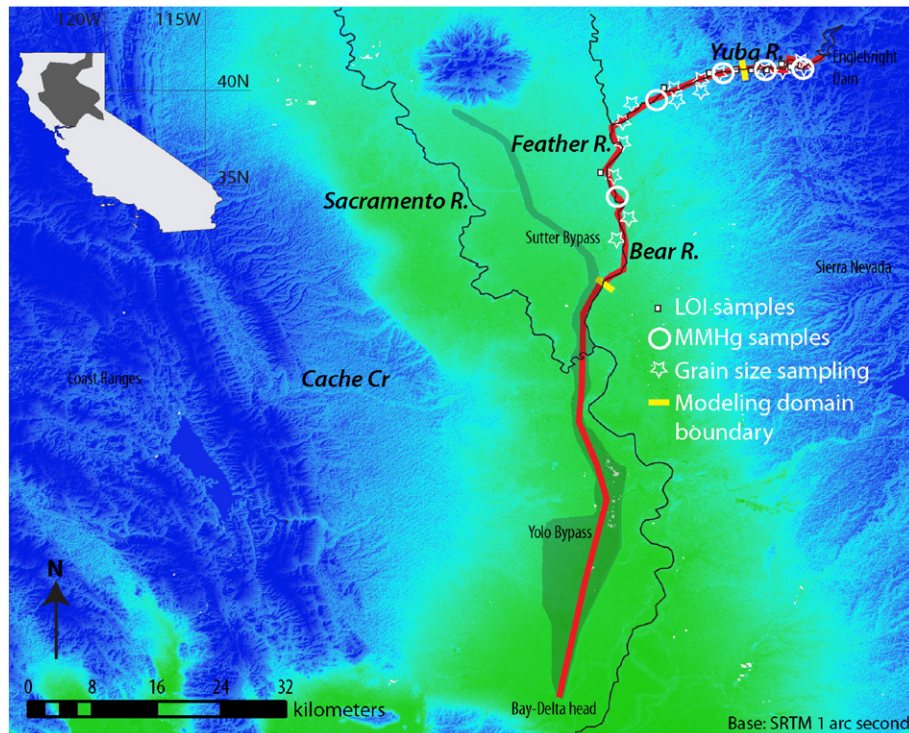

Fig. 1. Study area along the Lower Yuba and Feather Rivers showing the sampling transect (red), sites where biota were sampled for MMHg analysis (white ovals), where sediment was sampled for grain size (white stars) and LOI (white squares), and the boundaries of the modeling domain (yellow lines). Inset map of California shows the Sacramento River basin. Background colors indicate elevation where cooler colors are higher elevation (from 1-arc-second SRTM).
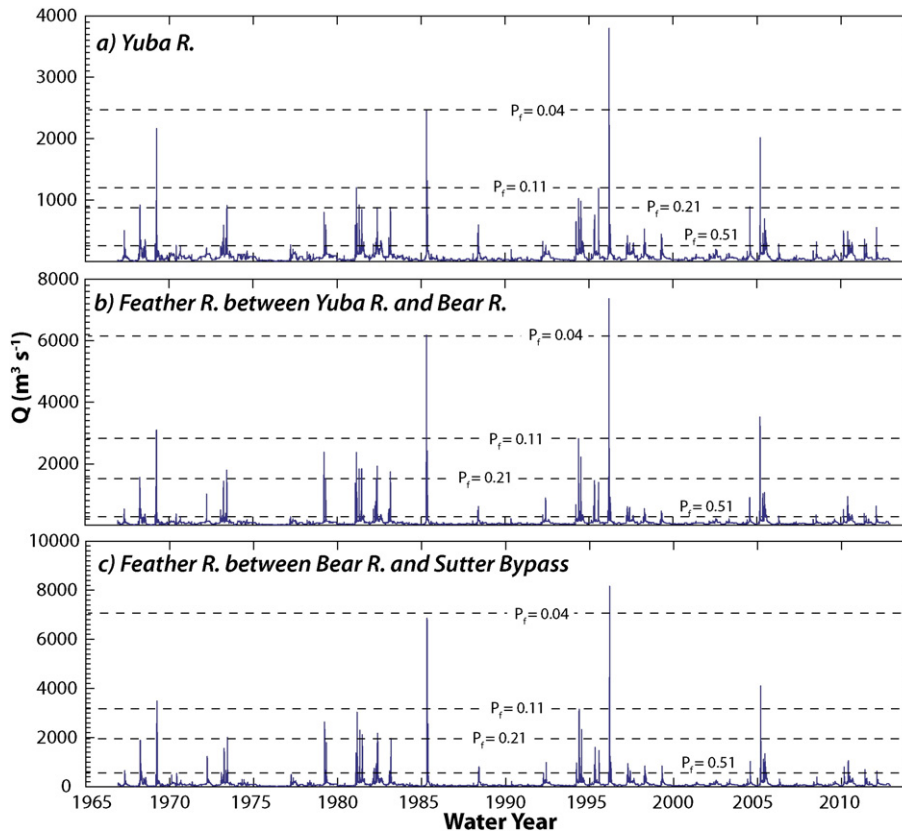
Fig. 2. Daily discharge series for each sector studied: Yuba R. (a), Feather R. between Yuba R. and Bear R. (b), and Feather R. between Bear R. and Sutter Bypass (c) for water year 1968–2013. Characteristic flood exceedance probabilities are indicated on each.

(Moir and Pasternack, 2010; Pasternack et al., 2010). There are ongoing projects designed to improve the physical habitat for these fish by altering the sediment dynamics and hydraulics, yet a major outstanding question is whether the widespread contamination previously documented in the study area could prove a risk to upper trophic organisms that prey on these migratory salmonids (e.g., waterfowl and humans). In this paper, we investigate hydrologically controlled MMHg production at the landscape scale.

3. Methods

This interdisciplinary research consisted of statistical analysis of hydrologic records, hydraulic modeling of inundation under various flows, creation of flood maps, analysis of cumulative inundated areas, consideration of THg, MMHg, and reactive Hg (HgR) measurements in biota and sediment, and simple calculations to estimate the MMHg production potential within sediment during inundation.

We used river channel cross sections extracted from a 1999 dataset of 0.6-m resolution LiDAR tied to channel bathymetry along the Lower Yuba and Feather Rivers (Figs. 1 & 3) that were provided by the US Army Corps of Engineers within the HEC-RAS hydraulic modeling framework, v.4.1 (http://www.hec.usace.army.mil/software/hec-ras/documentation.aspx). The upstream extent of our study area is in the middle of the Lower Yuba's course between Englebright Dam and the Feather River confluence in order to coincide with publicly available data on hydraulics and floodplain topography. In order to develop a seamless dataset for evaluation of inundation frequency and duration over the daily historical time series of post-dam streamflow (Water Years 1968–2013), we then routed historical flow under steady conditions through these cross sections via HEC-RAS using mean daily flow data over the same period (WY 1968–2013) from three upstream US

Geological Survey gauging stations: Yuba R. below Englebright Dam (Site#: 11418000, Latitude 39°14′07″, Longitude −121°16′23″), Feather R. at Oroville (Site#: 11407000, Latitude 39°31′18″, Longitude −121°32′48″), and Bear R. near Wheatland (Site#: 11424000, Latitude 39°00′01″, Longitude −121°24′20″). Daily flood frequency exceedance probabilities (P_f) for each of these stations were derived based on daily occurrence over the entire post-dam hydrologic record (P_f = 0.02, 0.04, 0.11, 0.21, 0.51, 0.74, 0.98).

Using an existing HEC-RAS hydraulic model developed by the Army Corps of Engineers for the entire Sacramento River basin (provided by Scott Stonestreet, USACE Sacramento), we performed a suite of steady flow simulations with varying recurrence intervals (1–100 years), corresponding to the P_f values above, on the Yuba and Feather Rivers. HEC-RAS solves the energy equation to obtain the water surface elevation between cross sections, and predicts that any location in the channel or floodplain is inundated if the predicted water surface elevation is greater than the local land-surface elevation. The HEC-RAS channel geometry contains cross-sections with a mean spacing of ~300 m. Bathymetric input data defining the wetted channel in the 1999 data was obtained via sonar scans, while the bank and floodplain topography was derived by the US Army Corps of Engineers from more detailed topographic data collected using aerial LiDAR (Stonestreet and Lee, 2000). The inundation extent of each flow discharge was calculated using the HEC-GeoRAS extension in ArcGIS. This involved exporting the water surface elevation values for each simulated flow from HEC-RAS, and subtracting them from a DEM of the riverbed and floodplain topography. The output includes raster maps of water depth (1 m cell sizes) and bounding polygons of the water surface extent.

We extracted from these output data flood maps in HEC-GeoRAS and analyzed the extent of inundated area associated with each inundation frequency probability. We also investigated the duration of flood events from the historical streamflow records by calculating the
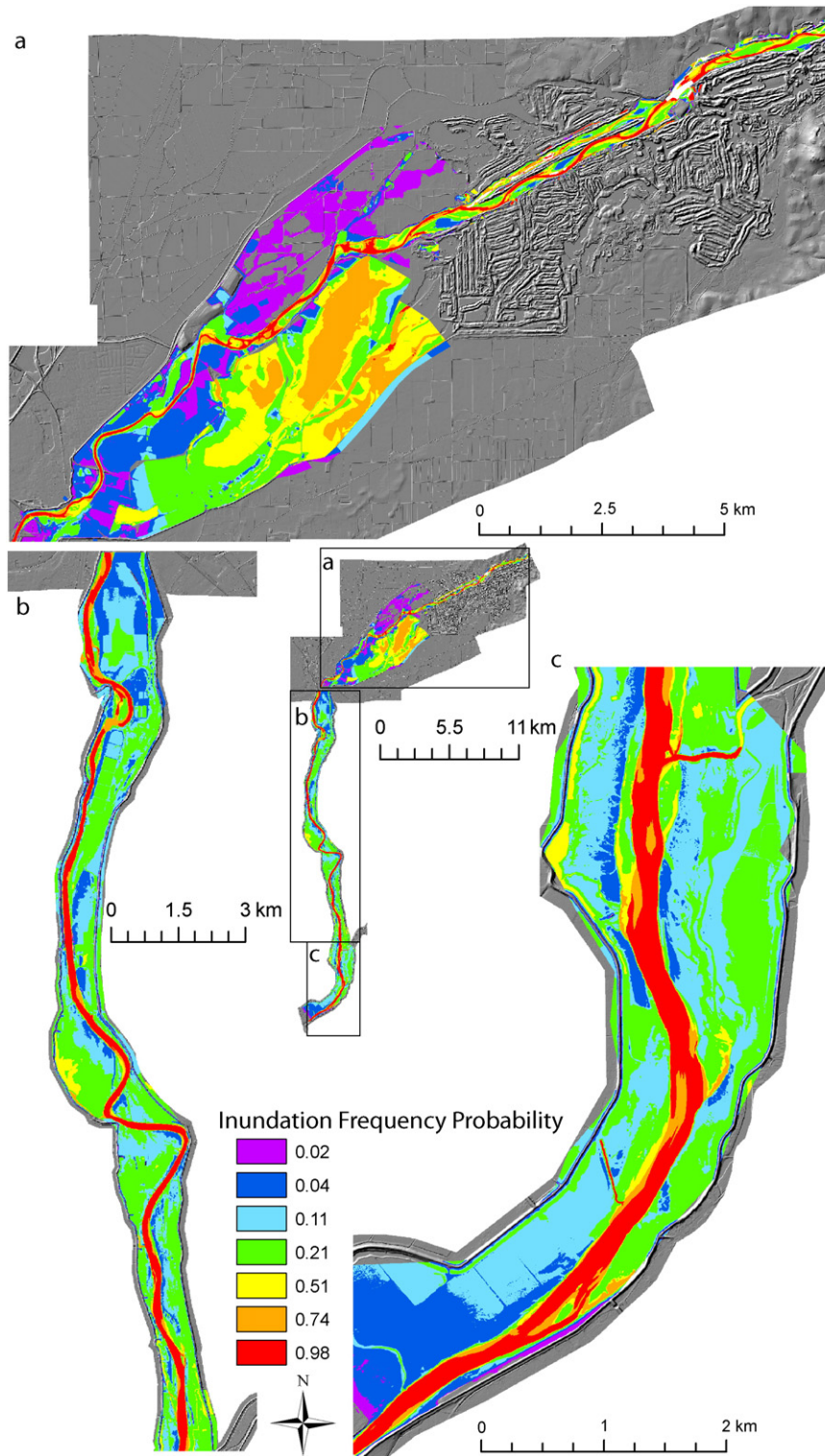
Fig. 3. Daily inundation frequency probability maps for three sectors of the Yuba-Feather system (see inset in center of figure): Yuba R. (a) and Feather R. between Yuba R. and Bear R. confluences (b) and Feather R. between Bear R. confluence and Sutter Bypass (c). These maps show the spatial extent for modeled steady flows at each empirically derived frequency probabilities.

probability of consecutive-day inundation durations of 2 days, 5 days, 10 days, and 20 days. For both inundation frequency and consecutive-day inundation, we use computed probabilities and areas in order to normalize the inundation areas by the probability of their occurrence in the historical record. Thus, we characterize the cumulative area inundated for each exceedance probability for both the Yuba and Feather Rivers. In addition to the Yuba sector, the Feather was separated into two sectors to account for the contributions of downstream tributaries: Feather R. between Yuba R. and Bear R. confluences (Fig. 3b) and Feather R. between the Bear R. and Sutter Bypass (Fig. 3c).

In order to better understand the local transformation from sediment-adsorbed iHg to MMHg, we analyzed two Hg species at the

USGS Hg laboratory in Menlo Park, CA. First, we measured MMHg (dry wt. concentration) in the <63 μm fraction of sediment and in non-migratory biota at various trophic levels (filamentous algae, caddis fly larvae, stone fly larvae, mayfly larva, aquatic worms, clams, forage fish) by HNO_3 extraction and ethylation. These samples were collected in flowing water (riffle environments) along Yuba and Feather Rivers in 2013 and 2014 (see Donovan et al., 2016 for collection and sample preparation details). At each sampling location, individual organisms were removed with clean, stainless steel tweezers, identified (to order, family, or species), sorted into composite samples (typically at least 10 individuals per sample), and immediately frozen on dry ice. Biotic samples were freeze-dried and ground with either an agate mortar and pestle or an alumina ball mixer mill prior to MMHg analysis. They represent MMHg accumulation in the local food web. MMHg was analyzed on a Brooks-Rand GC-CVAFS MMHg analyzer using EPA Method 1630. As reported elsewhere (Donovan et al., 2016), the relative percent deviation (RPD) of analytical duplicates for sediment was ±8.4% (n = 1 pair) and matrix spikes recovery was 107 ± 1% (n = 2) and certified reference material ERM-CC580 (estuarine sediment) recovery was 95% (n = 1). The RPD of analytical duplicates for biota was ±3.0% (n = 12 pairs), matrix spike recovery was 105 ± 5% (mean ± SE, n = 26). Recovery of MMHg from SRM NRC Tort-3 (lobster) was 86 ± 6% (mean ± SE, n = 7) and from NIST SRM 2967 (marine mussel tissue) was 93 ± 9% (mean ± SE, n = 7).

We also assayed 'reactive' mercury (HgR) in the fine (<63 μm; sieved) fraction of collected sediment (n = 44), a subset of samples previously analyzed for THg (see Singer et al., 2013 for details). These samples were collected in dry, oxic conditions from bank exposures and river terraces along the Yuba-Feather system at various depths. HgR has been methodologically defined as the fraction of THg, in samples that have not been chemically altered (for example, digested, oxidized, or chemically preserved), that is readily reduced to elemental Hg(0) by an excess of $SnCl_2$ under O_2-free (N_2 flushed) conditions over a set exposure time. This operationally defined parameter was developed as a surrogate measure of the fraction of iHg that is most likely available to bacteria responsible for MMHg production (Marvin-DiPasquale et al., 2009a; Marvin-DiPasquale and Cox, 2007). The reporting limit for HgR data was <2 ng g^{-1} and the RPD of all analytical duplicates was 4.2 ± 2.2% (n = 7 pairs).

Finally, to investigate the potential for MMHg production from Yuba and Feather R. sediment during inundation, we made first-order calculations to estimate MMHg production potential (MPP) under different inundation frequencies and consecutive-day durations extracted from the decadal streamflow history. We note that the actual values we calculate for MPP may be imprecise estimates, but in this paper we seek to explore the relative effects of flood frequency and inundation on MPP, rather than to obtain accurate values of MMHg production. Furthermore, we are not computing Hg flux into the food web, but rather generating estimates of gross methylation potential based on the best available information. We calculated MPP (g d^{-1}) in the following way. First, we generated a set of 44 HgR (ng g^{-1}) measurements in the laboratory from sediment (see above) along the Yuba (n = 25), Feather R. b/w Yuba and Bear (n = 14) and Feather R. below Bear (n = 5) sectors. Next, we obtained rate constants for microbial Hg(II) methylation (k_{meth}) rates (d^{-1}) based on an existing relationship between k_{meth} and percentage organic material in sediment obtained by loss-on-ignition (%LOI), which was developed in a previous study for observations in riverine sediments from other basins (Marvin-DiPasquale et al., 2009b):$\log(k_{meth}) = 1.53 * \log(\%LOI) - 3.97$, n = 90; $R^2 = 0.45$. We conducted LOI analysis (ActLabs, Ontario, Canada) on a subset of the original archived sediment samples used in our prior study (Singer et al., 2013), which spanned a range of geomorphic units in the river corridor. The average value of %LOI from analyzed samples collected at various locations along the channel and floodplains of the Yuba-Feather system was 7.6 ± 0.8% (mean ± SE, n = 13).

We partitioned the inundated area into riverbed and floodplain, each of which had different k_{meth} values. We then used these computed k_{meth} values to calculate methylmercury production potential over several decades (time-integrated MPP in g) as a function of HgR: $MPP = HgR - HgR * \exp(-k_{meth} * t)$, where t is time in days. To make this calculation, we used mean values of HgR obtained for the <63 μm fraction of sediment samples for each river sector, and also computed standard errors in the HgR values (and %LOI) for each sector, which were propagated through MPP results to obtain estimates of uncertainty. We assumed an average bulk density of 2.0 g cm^{-3}, for the riverbed and a value of 1.4 g cm^{-3} for the floodplain (wet sand with gravel and dry loose sand, respectively: http://www.engineeringtoolbox.com/density-materials-d_1652.html). We computed average percentages of the total grain size distribution comprised by the <63 μm sediment fraction separately for riverbed and floodplain samples. We sieved 7 riverbed samples and 8 floodplain samples along the lower Yuba and Feather Rivers (Fig. 1) in sufficient quantities to ensure the largest particle made up no more than 1% of the total mass, which is a more stringent standard than prior boat-based efforts in the Sacramento Valley (Singer, 2008a; Singer, 2008b; Singer, 2010). Assuming there is low spatial grain size variation within a particular geomorphic unit (riverbed v. floodplain), we averaged samples by unit to obtain a characteristic regional fraction of sediment <63 μm for channel (0.6 ± 0.4%, mean ± SE) and floodplain (45.6 ± 7.0%, mean ± SE) sediment to use in our MPP calculations. Finally, we restricted our computations of MPP in both channel and floodplain sediment to the upper 2 cm of depth below the surface, which is consistent with the depth in which k_{meth} values, used in the regression with LOI, were calibrated (Marvin-DiPasquale and Agee, 2003; Marvin-DiPasquale et al., 2009a). Thus, we obtain a conservative estimate of MPP based solely on inundation frequencies and durations produced by our hydraulic modeling (see Supplementary material for detail on the MPP calculations). These estimates are designed to simulate the retrospective impact of the decadal flow history on the existing in situ mercury-laden sediment along these sectors. MPP represents gross MMHg production, rather than flux into the environment. A significant percentage of any produced MMHg is likely to demethylate and/or become trapped within the sediments, rather than to enter local food webs (Gray et al., 2004a; Marvin-DiPasquale and Oremland, 1998).

Our goal was to obtain estimates of MPP based on available information, and we recognize that this calculation is poorly constrained in the best of circumstances due to process heterogeneity, and that it is a great challenge to assess MPP on the landscape scale. Thus, we present several caveats and assumptions here: 1) The depth of Hg-contaminated sediment varies throughout each sector, but we conservatively assess the MMHg production potential only in the upper 2 cm of depth profiles, and we assume sediment becomes water-logged during inundation. This estimate of shallow, inundation-driven methylation excludes MPP associated with subsurface hyporheic saturation, which is likely an important component of total MPP in river corridors. 2) Hg(II)-methylation only occurs during fully flooded conditions and no MMHg production occurs when the floodplain is not fully saturated. 3) MMHg production only occurs from HgR (a small percentage of iHg) within sediment <63 μm. 4) We compute MMHg production separately for channel and floodplain sediment, such that total inundated areas are partitioned in the MPP calculations. Since the percent of sediment <63 μm is very small for channel sediment, the channel does not contribute much to the total MPP calculations. 5) The approach used to estimate MPP is limited by the fact that we do not take into account the actual ambient chemistry or activity of the local microbial community at our sites, as these were not directly assessed in the current study. As such we have likely estimated an upper bound on gross MPP in surface sediment (which is why we use the term 'potential'). 6) Our spatial quantification of inundation areas and MPP values is limited to the lower part of the Yuba River that was modeled, and therefore excludes the contribution from highly contaminated sediment at sites upstream

of the Yuba Gold Fields (Singer et al., 2013). 7) Based on our measurements, we are assuming that there is sufficient available HgR in all inundated areas to enable MMHg production consistently over the entire decadal period. This may not be the case due to variability in the temporal and spatial distribution of Hg-laden sediment deposits in this system (and presumably in the HgR percentage), so in this respect our calculations represent an upper bound on MPP. 8) We are computing gross methylation potential, which is not a flux of MMHg into the environment because demethylation will counteract this MMHg production (Gray et al., 2004a; Marvin-DiPasquale and Oremland, 1998).

In spite of these caveats and assumptions, we believe this approach gives us reasonable estimates of MPP associated with various conditions of inundation. As such, significant differences in MPP between inundation scenarios provide insight into temporal and spatial variability in MMHg that are reflective of the hydrologic controls on redox state (i.e., loss of oxygen associated with replacement of water for air in sediment pore spaces and subsequent exhaustion by aerobic microbes).

4. Results

4.1. Flood maps

Flood maps produced by the hydraulic modeling of inundation frequency and consecutive-day duration are shown in Figs. 3–5. Fig. 3, daily inundation frequency, illustrates a constrained zone of inundation along the main channels of the Yuba and Feather during frequent ($P_f \geq 0.98$) flooding. These flows are entirely contained within the channel, so there is no additional floodplain inundation at this flow frequency. At flood probabilities of $P_f \leq 0.21$, a significant swath of floodplain becomes inundated along both Yuba and Feather Rivers, and the inundated area increases with decreasing flood probability such that the largest floods cover the most floodplain area. The inundated floodplain area for the $P_f \leq 0.02$ along the Feather is nearly indistinguishable from that of the $P_f \leq 0.04$ event, which floods the entire floodplain between bounding flood control levees (visible as the limits of flooding on Figs. 3b & 3c). However, there are significant areas of the Yuba R. floodplain that are inundated during the $P_f \leq 0.02$ flow (purple on Fig. 3a), but not during the $P_f \leq 0.04$ flow (dark blue) and widespread inundation occurs in this sector for flows as small as $P_f \leq 0.74$. Figs. 4 and 5 show a declining area of inundation with successively longer consecutive inundation periods for the Yuba R. and the Feather R., respectively, where most of the area decrease occurs between 5-day and 10-day periods (between b and c on both figures). The Feather floodplain essentially has a zero probability of being inundated for durations of 10 days or longer (apart from some small topographically low areas near the levees), while there are significant areas of the Yuba floodplain that remain flooded for up to 20 consecutive days (Fig. 4d). These areas are topographically low with very small drainage gradients that essentially behave as temporary wetlands during large flood events.

4.2. Inundation frequency

Figs. 6 and 7 show the translation of these inundation maps into bar charts to better illustrate the relationships between flood frequency, duration, and area. Fig. 6a shows the progressive decline in inundated area with increasing flood probability for all sectors studied. The Feather River sectors (red and yellow) exhibit notable declines in inundated area between $P_f \leq 0.11$ and $P_f \leq 0.51$. These transitions represent the threshold between floodplain-channel versus channel-only inundation (Fig. 3b and c). It is perhaps more insightful to normalize the inundated areas by daily inundation frequency probability, which allows for identification of flows of a particular frequency that are responsible for inundating the most area over the entire historical time series. This step reveals that while the highest normalized inundated area occurs at the highest frequency probability for both Feather River sectors, the
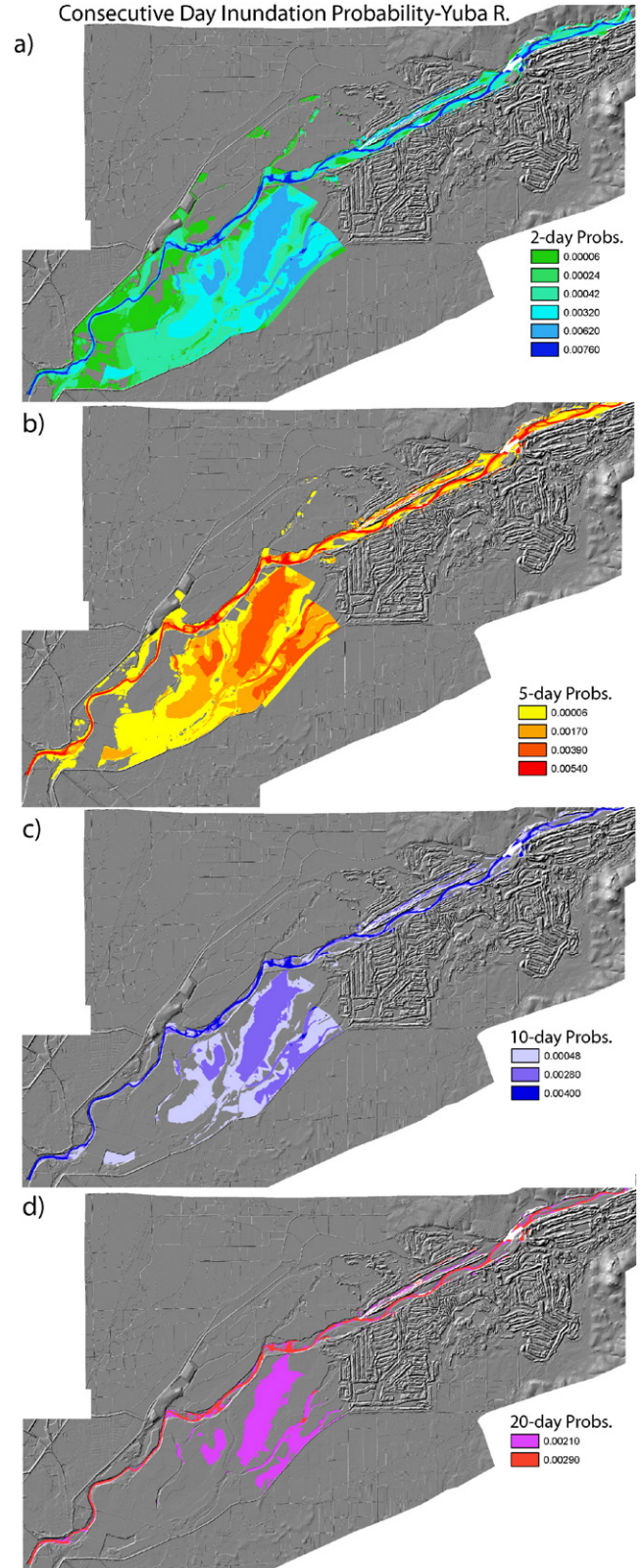

Fig. 4. Consecutive-day inundation duration probability maps for Yuba River for 2 days (a), 5 days (b), 10 days (c), and 20 days (d). These maps and those in Fig. 5 were generated by computing probabilities for the decadal time series of areas flooded for consecutive days (i.e., during the same flow).
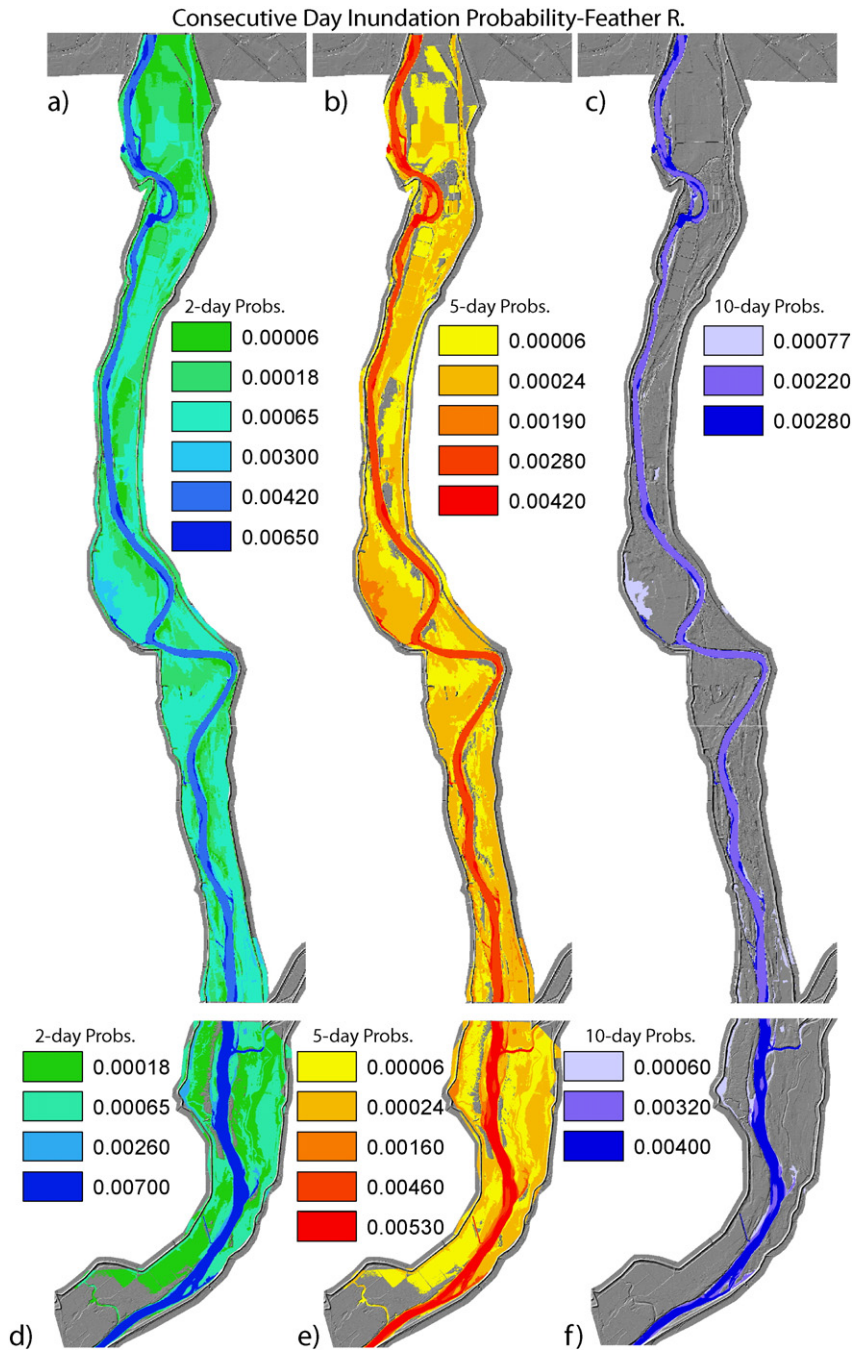
Fig. 5. Consecutive-day inundation duration probability maps for Feather River between the Yuba R. and Bear R. confluences for 2 days (a), 5 days (b), 10 days (c), and for the Feather R. between the Bear R. and Sutter bypass 2 days (d), 5 days (e), 10 days (f). Note: The probability categories for the most downstream reach of the Feather are different from those upstream, even though the legend colors are similar. The color values here also differ from those in the Yuba R. (Fig. 3).

$P_f \leq 0.51$ frequency flood produces the most inundated area for the Yuba R. (Fig. 6b), suggesting the potential importance of such median flows in biogeochemical processes such as methylation along that sector. It also reinforces the short-lived nature of overbank flows in the Feather R. sectors.

4.3. Inundation duration

Fig. 7 shows stacked bar charts of inundated area and probability-normalized inundated area within various bins of consecutive-day inundation probability for three values of consecutive-day duration (2-day, 5-day, and 10-day). For Fig. 7, the x-axis refers to the historical

likelihood of inundation for at least Z consecutive days, where Z is the duration listed at the top of each vertical pair of subplots. The height of each bar color indicates each sector's total area and its relative contribution to inundated area for each likelihood bin of inundation. For example, we can see that for the 2-day flood period, the largest overall area of inundation (and individually for both Yuba R. and Feather R. below Bear R. sectors) occurs at a 0.0007 probability (Fig. 7a). As the probability increases or decreases, the inundated area tails off, while the largest overall area of inundation occurs at the lowest probability for both 5-day and 10-day events (Fig. 7b and c). It is important to point out that the highest overall area for all three sites does not correspond directly with the highest area for any particular sector. For
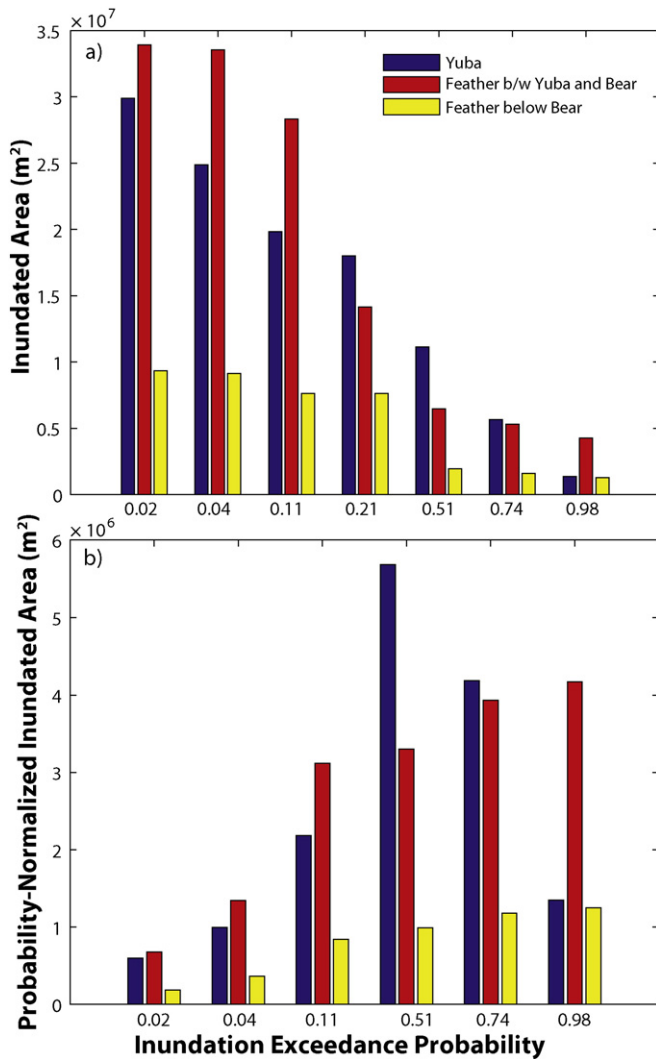
Fig. 6. Bar charts of area of inundation (a) and probability-normalized area (b) versus inundation frequency probability for the three sectors of the study area. Inundated areas were extracted from HEC-GeoRAS coverages in ArcGIS and were normalized by their empirical frequency probabilities.

example, the overall inundated area for the 10-day duration event peaks at $P_f \le 0.002$ for the Feather b/w Yuba R. and Bear R. and at $P_f \le 0.004$ for Feather below Bear (Fig. 7c), suggesting a different local relationship between flow and channel-floodplain topography within each sector of the river system. Namely, there is a higher probability of inundating more area for 10 consecutive flood days for the lower sector of the Feather than the upper sector due to lower topographic channel slopes where the river approaches a natural flood basin in the Sacramento Valley (Singer et al., 2008). Finally, total inundated area over the study basin generally decreases with consecutive-day flood duration (c.f. Fig. 7a–c) because increasingly longer floods are less common in the historical record (from 74 km² to 48 km² to 18 km² to 12 km², respectively for 2-day, 5-day, 10-day, and 20-day inundation durations).

As was the case for the frequency analysis, the normalized areas of consecutive-day duration (Fig. 7d–f) provide more information because they condition the area by the number of days over the entire historical period (WY 1968–2013) that it is actually inundated. The highest normalized inundation area occurs at a higher probability than the raw inundated areas for all three flood durations within the Yuba-Feather system. It also occurs at a higher probability for all sectors individually for 2-day and 5-day flood durations (c.f., Fig. 7a & d; b & e), as well as

for the Yuba R. and Feather R. below Bear R. sectors for the 10-day duration (Fig. 7c and 7f). The total normalized inundation areas also decline with duration for each sector and for the entire system (e.g., from 0.1 km², 0.06 km², 0.04 km², and 0.02 km² for the respective 2-day, 5-day, 10-day, and 20-day consecutive durations). Furthermore, these areas decline in the downstream direction by sector, with the exception of the 2-day consecutive duration flood. This latter inundation period produces three times more inundation area (both raw and normalized) in the Feather below Bear than it does for the Feather between the Yuba R. and Bear R., again perhaps due to the local decrease in slope where the Feather R. meets Sutter Bypass, which promotes more overbank flow with slower drainage over longer time periods.

4.4. Mercury species

Fig. 8 shows the MMHg in sediment and its bioaccumulation in the food web of the Yuba-Feather system. The mean MMHg concentration was 111.0 ± 16.8 ng g⁻¹ (mean $\pm$ SE, n = 31) for non-algal biota, 8.7 ± 1.1 ng g⁻¹ (mean $\pm$ SE, n = 12) for algae, and 5.2 ± 0.4 ng g⁻¹ (mean $\pm$ SE, n = 4) for sediment. The data have been separated by organism type and listed in order from low to high mean MMHg concentrations (Fig. 8) and %MMHg values were calculated for a subset of these biota in a separate study document a strong trend of MMHg bioaccumulation and trophic transfer in this aquatic system (Donovan et al., 2016). Donovan et al. (2016) also provided new isotopic evidence that MMHg may be produced within stream channels and taken up into filamentous algae and benthic macroinvertebrate species (e.g., insect larva, aquatic worms, Asian clams). These organisms are potential food sources to resident forage fish, which have the highest body burdens of Hg in this study, as well as other resident (e.g., rainbow trout) or migratory (e.g., salmonid) fish species. If microbial transformation within riverine and floodplain sediment is the primary source of MMHg production delivered to the base of the food web, it likely occurs over a broad area when there is sufficient expansion of flow into the floodplain to enable activity of anaerobic bacteria. Some proportion of the MMHg thus produced could then drain back into the main river channels on the falling limb of the hydrograph, where it would become available to aquatic biota.

It is likely that only a very small fraction of THg within gold mining sediment is available for methylation (Fleck et al., 2011; Marvin-DiPasquale et al., 2011; Marvin-DiPasquale and Cox, 2007). The operationally defined HgR assay approximates how much THg (Fig. 9a) is actually 'reactive' and thus potentially available to bacteria for microbial iHg methylation under optimal conditions. Our analyses of HgR in the <63 µm fraction of sediment in the Yuba-Feather system reveal an approximately order-of-magnitude range in HgR concentrations in this system with no evident downstream trend (Fig. 9b). The mean value was 11.8 ± 2.2 ng g⁻¹ (mean $\pm$ SE, n = 24) for the Yuba R. and 11.2 ± 1.4 ng g⁻¹ (mean $\pm$ SE, n = 18) for the Feather R., so the HgR concentration in sediment along both rivers is not statistically different (Kolmogorov-Smirnov, KS, test: $\alpha = 0.05$; $p = 0.8224$). We found no strong spatial gradients in HgR%, apart from a non-significant decline in Feather River sediment downstream of the Bear confluence (Fig. 9c). The mean HgR% value was $3.7 \pm 0.5\%$ (mean $\pm$ SE, n = 24) for the Yuba R. and $3.4 \pm 0.5\%$ (mean $\pm$ SE, n = 18) for the Feather R., again statistically indistinguishable (KS test: $\alpha = 0.05$; $p = 0.8630$). The only deviation is that samples from the Yuba Gold Fields (yellow) are relatively low in HgR and %HgR, which is ostensibly a consequence of intensive dredge mining for gold in this area that has diluted these samples of Hg.

4.5. Methylmercury calculations

Results from our MPP calculations are displayed in Fig. 10 (and detailed in Supplementary material). Since the calculations for inundation frequency (Fig. 10a) are multiplied by the number of days in which they
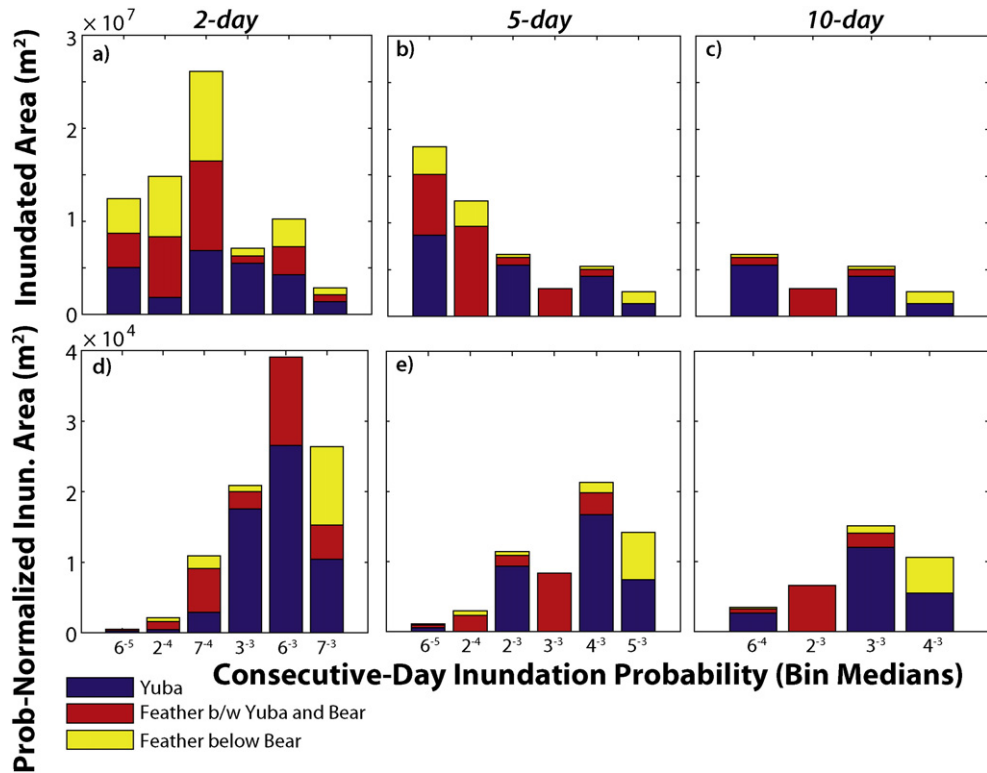
Fig. 7. Stacked bar charts of inundated area versus consecutive-day inundation probability for 2-day (a), 5-day (b), and 10-day (c) durations; and probability-normalized inundated area versus consecutive-day inundation probability for 2-day (d), 5-day (e) and 10-day (f) durations. Areas were extracted from HEC-GeoRAS coverages in ArcGIS and were normalized by the computed probabilities.

occurred in the historical hydrologic record (Fig. 2), they are indicative of normalized rates of MMHg production potential, similar to the patterns shown in Fig. 6b. By these estimates, discharges approximating the median frequency flow ($0.21 < P_f \leq 0.51$) potentially generated ~20.1 ± 3.9 kg (mean $\pm$ SE) of MMHg from contaminated Yuba R. sediment and a total of ~14.6 ± 2.9 kg (mean $\pm$ SE) from Feather R. sediment (both sectors) over the period 1967–2013 (total of 5040 days). In contrast, discharge equaling or exceeding the largest flow studied ($P_f \leq 0.02$) generated MPP of only ~3.6 ± 0.7 kg (mean $\pm$ SE) within

the Yuba and 5.0 ± 1.0 kg (mean $\pm$ SE) over the same decadal period (total of 336 inundation days). This highlights differences in the spatiotemporal patterns of large, infrequent flows between the Yuba and Feather Rivers (Figs. 3 & 6) and their potential impact on MMHg production potential. For example, the highest total MPP along the Feather R. (both sectors) over the historical post-dam time series is estimated to have occurred during relatively high flows with $P_f \leq 0.21$, whereas for the Yuba R. it occurred for flows only exceeding the median value ($P_f \leq 0.51$). Summing up the MPP values over the entire decadal period
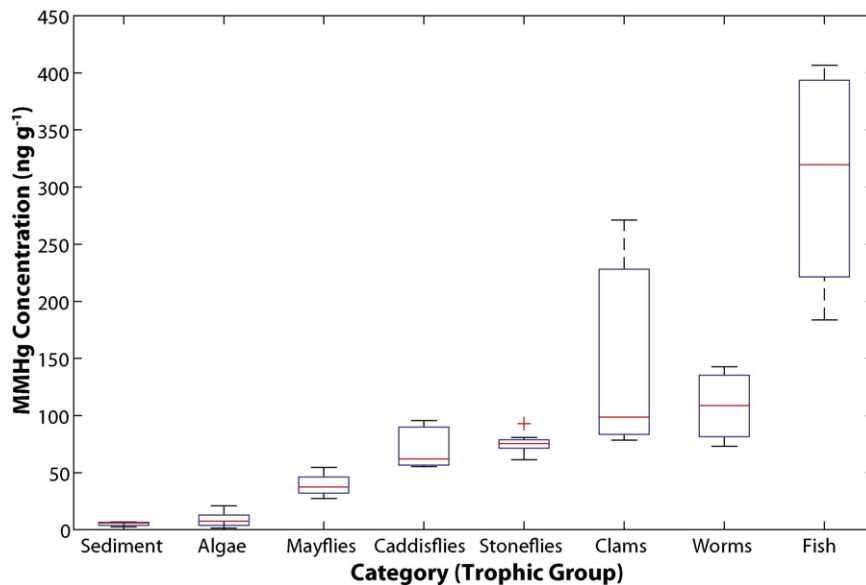

Fig. 8. Boxplots of MMHg (dry weight) in biota separated by organismal group for all samples in the Yuba-Feather system. Sampling locations are shown in Fig. 1. Sampling details provided in Donovan et al. (2016).
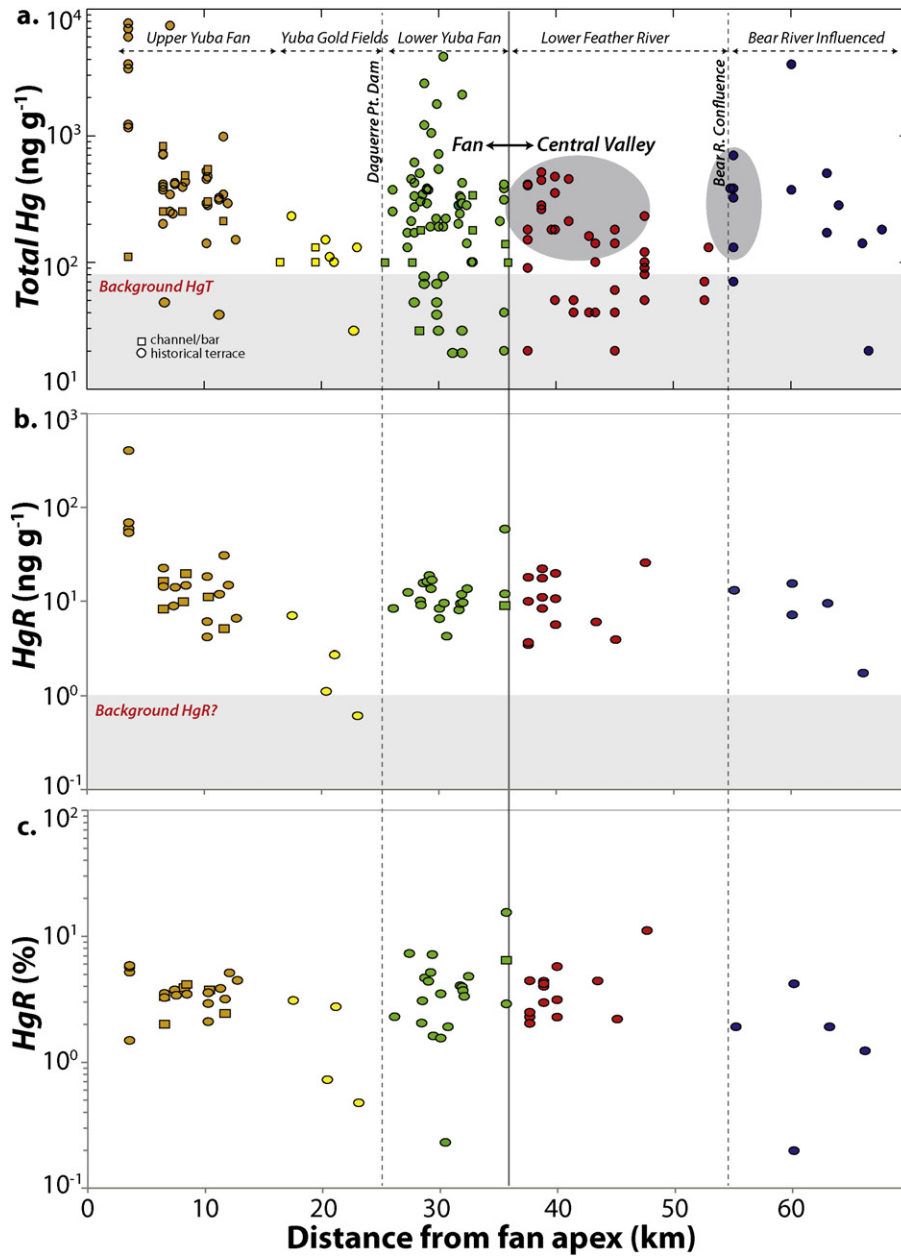
Fig. 9. Downstream trends in Hg species (distance downstream from Yuba Fan Apex): THg (a); HgR concentration (b); and HgR percentage of THg (c). Symbol colors refer to spatial domains listed at the top. Vertical solid line indicates the boundary between the Yuba Fan and the Central Valley, while the dashed lines refer to the locations of Daguerre Pt. Dam and the Bear R. confluence. The gray shaded area refers to inferred background (non-mining derived) values. Note: only HgR values from the Yuba Gold Fields and areas downstream were used for the MMHg production calculations.

of analysis, the Yuba generated the highest MMHg production potential of all these sectors (53.8 ± 10.5 kg), but both Feather River sectors combined have a higher total MPP (60.8 ± 12.0 kg), of which the Feather below Bear R. sector makes up only 21%. For comparison, total inundated area along the Yuba for $P_f \leq 0.02$ comprised ~30 km^2, while it made up ~43 km^2 for both sectors of the Feather (the Feather b/w Yuba and Bear made up 33.9 km^2 and the Feather below Bear comprised 9.3 km^2). These values are based on the approximate maximum values of inundation area for both rivers over the period of record (Fig. 6).

Fig. 10b shows MPP corresponding to the cumulative area inundated for events of each consecutive duration period. In contrast to the inundation frequency calculations, MMHg production potential is monotonically proportional to consecutive-day duration for the cumulative study area and for the Yuba R. in particular, where the highest MMP estimated was for the 20-day duration, even after accounting for the number of instances within the historical record in which these long-duration flows

occur (~49 times for the Yuba R., 35 times for the Feather R. b/w Yuba and Bear, and 54 times for Feather below Bear). These ~46 periods of 20-day inundation (~2.5 years in total) along both rivers are estimated to have generated 1.1 ± 0.2 kg of MMHg along both rivers, compared with the 0.5 ± 0.1 kg estimated to have been produced during all historical 2-day inundation periods (~119 periods in the historical record or ~0.7 years, depending on the sector), which were more limited to the near-channel area. Note that MPP for the 20-day duration is dominated by the Yuba sector, which contains large areas that stay inundated for such extended periods (Fig. 4). In contrast, MPP peaks for the Feather R. b/w Yuba and Bear at the 5-day duration, while it peaks for the Feather below Bear at the 2-day duration, which occurred ~71 times and ~118 times, respectively, between 1968 and 2013. These disparities in MPP are due to nonlinearity between flood recurrence interval and inundated area (Figs. 6 and 7), as well as lower methylation rates along the main channels due to a smaller percentage of grain sizes
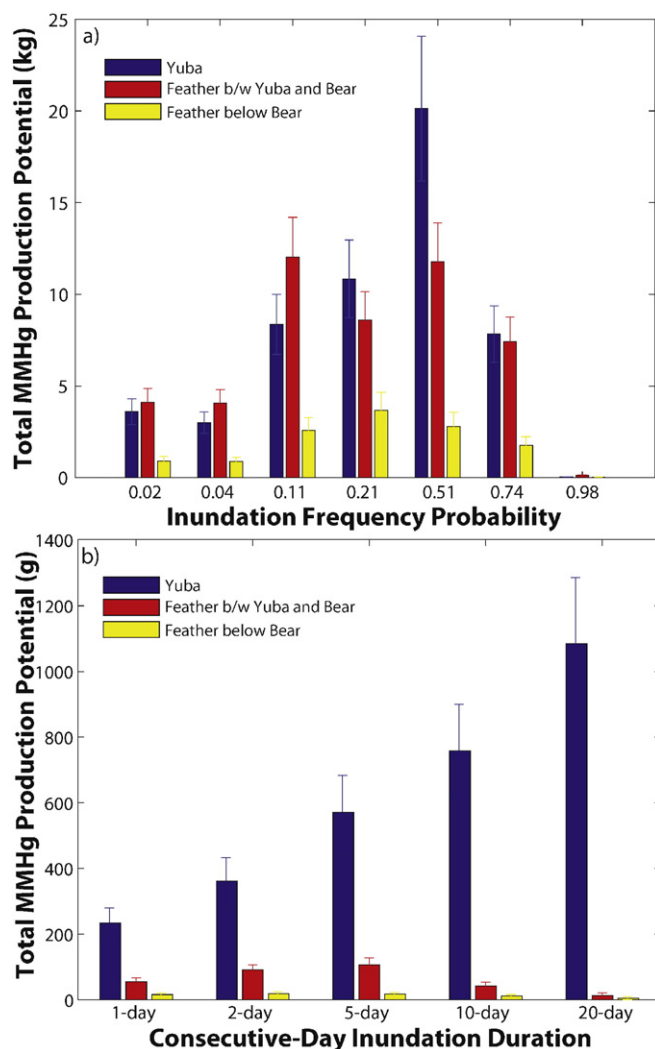
Fig. 10. Bar charts showing results of calculations of total MMHg production for Yuba and Feather Rivers for each inundation frequency probability (a) and results of calculations of total (cumulative over the entire historical flow record) MMHg production for areas of the Yuba and Feather Rivers for each consecutive-day inundation probability (b). Error bars represent standard error around the mean estimates based on variability in measured HgR.

finer than 63 µm. In other words, the Yuba gains MPP with longer durations due to increasing cumulative area of inundation, while the Feather loses MPP above a lower consecutive-day duration threshold because flow becomes restricted to the channel only.

5. Discussion

Redox sensitive metals such as Hg undergo changes in speciation in response to physical, chemical, and biological forcing. Such changes are modulated by initial sediment concentrations, sediment mineralogy, inundation history, and ambient chemistry. Many in situ factors may cause chemical changes in Hg speciation that can increase MMHg production (Compeau and Bartha, 1985; Marvin-DiPasquale et al., 2009b) at sites containing sediment-adsorbed Hg. These factors include redox fluctuation associated with temperature changes, wetting/drying cycles, and local chemistry (Benoit et al., 1999; Benoit et al., 1998; Gilmour et al., 1992; Schaefer and Morel, 2009; Wallschlager et al., 1998), most of which were not measured in this study. Nevertheless, we should expect spatial variability in gross MMHg production through fluvial networks that reflects the convergence of these factors. Indeed, recent research has demonstrated downstream increases in MMHg in

some river basins due to factors such as inundation history and groundwater drainage (Bradley et al., 2011; Bradley et al., 2012; Tsui et al., 2009a,2009b). In the Yuba-Feather system, the current sediment iHg values are high and ambient chemistry with respect to the labile fraction of Hg (HgR) appears to be nearly spatially uniform (e.g., Fig. 9b and c). If we assume that microbial communities responsible for methylation are approximately uniform in abundance and activity across a watershed, then inundation history remains an important variable that impacts spatial variability of gross MPP. Although we expect differences in non-hydrologic factors, the inundation history is likely a first-order driver of floodplain biogeochemistry because it controls many factors that influence redox conditions. Even when river waters are well oxygenated (mean dissolved oxygen value for Yuba River water 2000–2014 = 9.6 ± 1.5 mg L^{-1}; n = 4487, http://yubashed.org/viewdata/parameters/dissolved-oxygen), suboxic or anoxic zones commonly develop in pore waters due to low flow velocities (stagnation), weak pore connectivity, and long water residence times (Boulton et al., 1998; Briggs et al., 2015; Zarnetske et al., 2011). Remaining dissolved oxygen may then be consumed by aerobic respiration, which produces zones of anoxia within sediments (Vroblesky and Chapelle, 1994), and thus promotes activity of anaerobic microbes capable of Hg methylation.

Inundation history has indeed been shown to result in spatial variability of Hg biogeochemical processing (Gray et al., 2004a; Hudson-Edwards, 2003; Lindqvist et al., 1991; Mason et al., 1999), which may increase (Bonzongo et al., 2006) or decrease (Hurley et al., 1998; Ullrich et al., 2007) methylation potential during high overbank flows, depending on factors that have been well studied in lakes (e.g., Suchanek et al., 1998), but are less well understood in fluvial systems (Bradley et al., 2011; Bradley et al., 2012; Tsui et al., 2009b), even though there is a relatively large body of work on nitrate production in hyporheic zones (e.g., Briggs et al., 2014; Duff and Triska, 1990; Zarnetske et al., 2011). Recent work has identified unexpected Hg behavior in rivers, wherein there is high seasonal and spatial variability in MMHg (Choe et al., 2004; Conaway et al., 2003; Heim et al., 2007), and where Hg(II)-methylation increases during low flow periods following spring flooding until it reaches a peak and then declines (Tsui et al., 2009a).

Using several simplifying assumptions, this paper has investigated the potential for MMHg production over almost five decades based chiefly on spatial and temporal variability in flow history. We show that the area of floodplain inundation along the Yuba-Feather system increases monotonically with decreasing flood frequency (bigger, less frequent floods), which is no surprise because larger floods are more likely to flow over riverbanks into the floodplain, filling in topographically low areas. The area of inundation expands markedly at $P_f \leq 0.21$ for both rivers (Fig. 3), although substantial areas of the Yuba R. floodplain are inundated more frequently (at $P_f \leq 0.74$, Fig. 3a) as low points in the natural levee along the left bank of the Yuba allow flows to enter more often. Given the high frequency of inundation in this region of the Yuba R. floodplain, we consider these orange areas (Fig. 3a) as hot spots of MMHg production potential. There are also a few red areas of the Yuba R. and Feather R. floodplains that indicate locations of former channel positions (James and Singer, 2008; James et al., 2009), which remain topographically low. The green areas on Fig. 3 (both Yuba R. and Feather R. sectors) also represent potential hot spots, but since the frequency of inundation is considerably lower, estimated MMHg production potential is also relatively low (Fig. 10a); these zones may thus be considered only 'warm spots' of MPP. In contrast, extreme events ($P_f \leq 0.04$) cover massive areas and are often assumed to be very important to Hg methylation (Balogh et al., 2006) because they temporarily generate so much inundated area that the region appears like an inland sea (Kelley, 1998). However, since they are so infrequent and so short-lived (<2 days at a time, Figs. 4 and 5), they may have a relatively small impact on total estimated MMHg production over the long term (Fig.10a). In other words, the intersection of flow frequency and

inundated area is likely a more important determinant of a MPP hot spot than flood magnitude on its own.

The analysis of consecutive-day duration provides information on hot moments of potential MPP, insofar as Hg can be assumed to be generated more rapidly and efficiently during longer individual inundation periods (e.g., akin to a seasonal wetland). The Yuba R. floodplain contains areas, south of the river, which are inundated for as long as 20 consecutive days (pink areas on Fig. 4d). Notably, these low-lying areas exist within the same larger areas affected by the $P_f \leq 0.74$ flow frequency hot spot (Fig. 3a). Thus, these areas are doubly important as hot spots and hot moments of MPP. They should be considered high priority for future analysis of Hg speciation. There are far fewer hot moment locations along the Feather because it apparently drains much faster than parts of the Yuba R. floodplain. For example, the 2-day and 5-day flood durations do generate a large amount of inundated area along the channel (nearly levee-to-levee) in both sectors of the Feather R., but there are nearly no floodplain areas that flood for 10 consecutive days, apart from some former channel positions, which were also identified as hot spots (Fig. 5). The latter topographic lows may be considered hot moments, too, because they go through wetting and drying cycles, but remain inundated for periods apparently long enough to generate significant MPP (Fig. 10b). Once MMHg is produced, it is either demethylated in situ (Gray et al., 2004b; Marvin-DiPasquale and Oremland, 1998), trapped in sediments, transported into the channel during floodplain drainage, where it may easily be taken up into the aquatic food web (Balogh et al., 2006; Bradley et al., 2011; Hinkle et al., 2014), or it may percolate into phreatic aquifers, which is common at mountain fronts in the region (Meixner et al., 2016).

The HgR and MMHg data we have for the Yuba-Feather river system provide evidence that there is an abundance of relatively consistent amounts of reactive Hg adsorbed to sediment all along these river corridors, which may be easily methylated under suboxic or reducing redox conditions. This suggests that the legacy of hydraulic gold mining in the Yuba-Feather system continues to have a protracted impact on MMHg bioaccumulation in downstream food webs. Hg isotope data from a recent study suggest that contamination of resident aquatic organisms is most likely the result of in situ net methylation (difference of methylation and demethylation), rather than an upstream or external source (Donovan et al., 2016). The results presented here support such a hypothesis, and further suggest that MMHg production and bioaccumulation in the food web is likely to continue in the Yuba-Feather system as a result of flood pulses that inundate broad floodplain areas in spatial patterns that reflect topographic connectivity (Junk et al., 1989; Tockner et al., 2000; Trigg et al., 2013).

Storms which cause very heavy rainfall and significant basin-wide flooding are considered to be the driver of most major floods in California. So-called atmospheric rivers that produce high rainfall are likely to become more common under climate changes documented in California (Dettinger, 2011). Recent analysis has shown the duration of such floods has increased over the last several decades (Singer, 2007). These findings suggest that increased frequency and duration of regional floods capable of inundating the floodplain will have potentially important implications for MMHg production and MMHg bioaccumulation in regional food webs.

It must be noted that we have addressed the impact of surface inundation on methylation, but have ignored the subsurface. One important area for future work is analysis of the role of hyporheic flow in MMHg production, which has not been treated here. Furthermore, a major priority is to measure in situ methylation during flood conditions, which has been impossible during the recent California drought.

Finally, the results presented here have very important implications for migratory anadramous fish and their predators (including humans and waterfowl) in the Yuba-Feather system and beyond. Recent efforts have been undertaken to expand the range of migrating Chinook salmon from the San Francisco Bay-Delta to spawning sites along rivers in the Sierra foothills, such as the Yuba R., by altering the physical environment through gravel augmentation and regrading of bar forms (e.g., Moir and Pasternack, 2010; Pasternack et al., 2010), as well as by constructing increased connection for juvenile salmon to enter major river floodplains (Sommer et al., 2001). Given the contamination prevalent in sediment and biota in the sectors studied, coupled with continued MMHg production potential under flooding conditions within river floodplains, and past evidence of higher methylmercury concentrations in fish feeding in contaminated environments (Henery et al., 2010), caution should be exercised in plans to attract more anadromous fish to enter, feed, and spawn in any part of these contaminated riverscapes.

6. Conclusion

In this paper we show that analyses of both flood frequency and flood duration may be critical for assessing potential locations in the landscape where MMHg production is likely to occur frequently (hot spots) and episodically during long flood events (hot moments). We demonstrate significant biomagnification of MMHg in biota of the mining-contaminated Yuba-Feather River system and hydrologic indicators of this disproportionate role of long-duration flood events on MMHg production potential. Our results indicate the prolonged and ongoing long-term legacy of major mining operations on food web contamination. We highlight an important consideration with respect to restoration of salmon habitat restoration, especially under climate that is increasingly defined by drought-flood-drought cycles. More broadly, the analysis presented here establishes a framework for understanding the links between biogeochemical processing of contaminants in river floodplains at the landscape scale and over a period of decades.

Appendix A. Supplementary data

Supplementary data to this article can be found online at http://dx.doi.org/10.1016/j.scitotenv.2016.03.005.

References

Baldwin, D.S., Mitchell, A.M., 2000. The effects of drying and re-flooding on the sediment and soil nutrient dynamics of lowland river–floodplain systems: a synthesis. Regul. River. 16, 457–467.

Balogh, S.J., Swain, E.B., Nollet, Y.H., 2006. Elevated methylmercury concentrations and loadings during flooding in Minnesota rivers. Sci. Total Environ. 368, 138–148.

Benoit, J.M., Gilmour, C., Heyes, A., Mason, R.P., Miller, C., 2003. Geochemical and biological controls over methylmercury production and degradation in aquatic ecosystems. In: Chai, Y., Braids, O.C. (Eds.), Biogeochemistry of Environmentally Important Trace ElementsSymposium Series No. 835. American Chemical Society, Washington, D.C., pp. 262–297.

Benoit, J.M., Gilmour, C.C., Mason, R.P., Heyes, A., 1999. Sulfide controls on mercury speciation and bioavailability to methylating bacteria in sediment pore waters. Environ. Sci. Technol. 33, 951–957.

Benoit, J.M., Gilmour, C.C., Mason, R.P., Riedel, G.S., Riedel, G.F., 1998. Behavior of mercury in the Patuxent River estuary. Biogeochemistry 40, 249–265.

Beutel, M.W., Leonard, T.M., Dent, S.R., Moore, B.C., 2008. Effects of aerobic and anaerobic conditions on P, N, Fe, Mn, and Hg accumulation in waters overlaying profundal sediments of an oligo-mesotrophic lake. Water Res. 42, 1953–1962.

Blum, M., Gustin, M.S., Swanson, S., Donaldson, S.G., 2001. Mercury in water and sediment of Steamboat Creek, Nevada: implications for stream restoration. J. Am. Water Resour. Assoc. 37, 795–804.

Bonzongo, J.C.J., Nemer, B.W., Lyons, W.B., 2006. Hydrologic controls on water chemistry and mercury biotransformation in a closed river system: the Carson River, Nevada. Appl. Geochem. 21, 1999–2009.

Boulton, A.J., Findlay, S., Marmonier, P., Stanley, E.H., Valett, H.M., 1998. The functional significance of the hyporheic zone in streams and rivers. Annu. Rev. Ecol. Syst. 29, 59–81.

Bouse, R.M., Fuller, C.C., Luoma, S., Hornberger, M.I., Jaffe, B.E., Smith, R.E., 2010. Mercury-contaminated hydraulic mining debris in San Francisco Bay. San Francisco Estuary and Watershed Science Journal 8, 28.

Bradley, P.M., Burns, D.A., Murray, K.R., Brigham, M.E., Button, D.T., Chasar, L.C., et al., 2011. Spatial and seasonal variability of dissolved methylmercury in two stream basins in the Eastern United States. Environ. Sci. Technol. 45, 2048–2055.

Bradley, P.M., Journey, C.A., Lowery, M.A., Brigham, M.E., Burns, D.A., Button, D.T., et al., 2012. Shallow groundwater mercury supply in a coastal plain stream. Environ. Sci. Technol. 46, 7503–7511.

Briggs, M.A., Day-Lewis, F.D., Zarnetske, J.P., Harvey, J.W., 2015. A physical explanation for the development of redox microzones in hyporheic flow. Geophys. Res. Lett. 42, 4402–4410.

Briggs, M.A., Lautz, L.K., Hare, D.K., 2014. Residence time control on hot moments of net nitrate production and uptake in the hyporheic zone. Hydrol. Process. 28, 3741–3751.

Buckman, K.L., Marvin-DiPasquale, M., Taylor, V.F., Chalmers, A., Broadley, H.J., Agee, J., et al., 2015. Influence of a chlor-alkali superfund site on mercury bioaccumulation in periphyton and low-trophic level fauna. Environ. Toxicol. Chem. 34, 1649–1658.

Choe, K.Y., Gill, G.A., Lehman, R.D., Han, S., Heim, W.A., Coale, K.H., 2004. Sediment-water exchange of total mercury and monomethyl mercury in the San Francisco Bay-Delta. Limnol. Oceanogr. 49, 1512–1527.

Coleman Wasik, J.K., Engstrom, D.R., Mitchell, C.P.J., Swain, E.B., Monson, B.A., Balogh, S.J., et al., 2015. The effects of hydrologic fluctuation and sulfate regeneration on mercury cycling in an experimental peatland. Journal of Geophysical Research: Biogeosciences , n/a-n/a.

Compeau, G.C., Bartha, R., 1985. Sulfate-reducing bacteria: principal methylators of mercury in anoxic estuarine sediment. Appl. Environ. Microbiol. 50, 498–502.

Conaway, C.H., Ross, J.R.M., Looker, R., Mason, R.P., Flegal, A.R., 2007. Decadal mercury trends in San Francisco Estuary sediments. Environ. Res. 105, 53–66.

Conaway, C.H., Squire, S., Mason, R.P., Flegal, A.R., 2003. Mercury speciation in the San Francisco Bay estuary. Mar. Chem. 80, 199–225.

Creswell, J.E., Kerr, S.C., Meyer, M.H., Babiarz, C.L., Shafer, M.M., Armstrong, D.E., et al., 2008. Factors controlling temporal and spatial distribution of total mercury and methylmercury in hyporheic sediments of the Allequash Creek wetland, northern Wisconsin. Journal of Geophysical Research: Biogeosciences 113, G00C02.

Cristol, D.A., Brasso, R.L., Condon, A.M., Fovargue, R.E., Friedman, S.L., Hallinger, K.K., et al., 2008. The movement of aquatic mercury through terrestrial food webs. Science 320, 335.

Dettinger, M., 2011. Climate change, atmospheric rivers, and floods in California — a multimodel analysis of storm frequency and magnitude changes. JAWRA Journal of the American Water Resources Association 47, 514–523.

Domagalski, J.L., 1998. Occurrence and transport of total mercury and methyl mercury in the Sacramento River basin, California. J. Geochem. Exploration 64, 277–291.

Domagalski, J.L., 2001. Mercury and methylmercury in water and sediment of the Sacramento River basin, California. Appl. Geochem. 16, 1677–1691.

Donovan PM, Blum JD, Singer MB, Marvin-Di Pasquale M, Tsui MTK. Methylmercury degradation and exposure pathways in streams and wetlands impacted by historical mining. In Review.

Donovan, P.M., Blum, J.D., Singer, M.B., Marvin-DiPasquale, M.C., Tsui, M.T.K., 2016. Isotopic composition of inorganic mercury and methylmercury downstream of a historical gold mining region. Environ. Sci. Technol.

Donovan, P.M., Blum, J.D., Yee, D., Gehrke, G.E., Singer, M.B., 2013. An isotopic record of mercury in San Francisco Bay sediment. Chem. Geol. 349–350, 87–98.

Duff, J.H., Triska, F.J., 1990. Denitrifications in sediments from the hyporheic zone adjacent to a small forested stream. Can. J. Fish. Aquat. Sci. 47, 1140–1147.

Eagles-Smith, C.A., Ackerman, J.T., De La Cruz, S.E.W., Takekawa, J.Y., 2009. Mercury bioaccumulation and risk to three waterbird foraging guilds is influenced by foraging ecology and breeding stage. Environ. Pollut. 157, 1993–2002.

Fleck, J.A., Alpers, C.N., Marvin-DiPasquale, M., Hothem, R.L., Wright, S.A., Ellett, K., et al., 2011. The effects of sediment and mercury mobilization in the South Yuba River and Humbug Creek confluence area, Nevada County, California: concentrations, speciation and environmental fate — part 1: field studies. U.S. Geological Survey Open-File Report 2010–1325A.

Gehrke, G.E., Blum, J.D., Marvin-DiPasquale, M., 2011a. Sources of mercury to San Francisco Bay surface sediment as revealed by mercury stable isotopes. Geochim. Cosmochim. Acta 75, 691–705.

Gehrke, G.E., Blum, J.D., Slotton, D.G., Greenfield, B.K., 2011b. Mercury isotopes link mercury in San Francisco Bay forage fish to surface sediments. Environ. Sci. Technol. 45, 1264–1270.

Ghoshal, S., James, L.A., Singer, M.B., Aalto, R., 2010. Channel and floodplain change analysis over a 100-year period: lower Yuba River, California. Remote Sens. 2, 1797–1825. http://dx.doi.org/10.3390/rs2071797.

Gilbert, G.K., 1917. Hydraulic-mining debris in the Sierra Nevada. US Geological Survey Professional Paper 105, Menlo Park, CA.

Gilmour, C.C., Henry, E.A., Mitchell, R., 1992. Sulfate stimulation of mercury methylation in fresh-water sediments. Environ. Sci. Technol. 26, 2281–2287.

Gilmour, C.C., Podar, M., Bullock, A.L., Graham, A.M., Brown, S.D., Somenahally, A.C., et al., 2013. Mercury methylation by novel microorganisms from new environments. Environ. Sci. Technol. 47, 11810–11820.

Gray, J.E., Hines, M.E., Higueras, P.L., Adatto, I., Lasorsa, B.K., 2004a. Mercury speciation and microbial transformations in mine wastes, stream sediments, and surface waters at the Almaden Mining District, Spain. Environ. Sci. Technol. 38, 4285–4292.

Gray, J.E., Hines, M.E., Higueras, P.L., Adatto, I., Lasorsa, B.K., 2004b. Mercury speciation and microbial transformations in mine wastes, stream sediments, and surface waters at the Almadén Mining district, Spain. Environ. Sci. Technol. 38, 4285–4292.

Greenfield, B.K., Jahn, A., 2010. Mercury in San Francisco Bay forage fish. Environ. Pollut. 158, 2716–2724.

Greenfield, B.K., Melwani, A.R., Allen, R.M., Slotton, D.G., Ayers, S.M., Harrold, K.H., et al., 2013. Seasonal and annual trends in forage fish mercury concentrations, San Francisco Bay. Sci. Total Environ. 444, 591–601.

Grigal, D.F., 2002. Inputs and outputs of mercury from terrestrial watersheds: a review. Environ. Rev. 10, 1–39.

Heim, W.A., Coale, K.H., Stephenson, M., Choe, K.Y., Gill, G.A., Foe, C., 2007. Spatial and habitat-based variations in total and methyl mercury concentrations in surficial sediments in the San Francisco Bay-Delta. Environ. Sci. Technol. 41, 3501–3507.

Henery, R.E., Sommer, T.R., Goldman, C.R., 2010. Growth and methylmercury accumulation in juvenile Chinook Salmon in the Sacramento River and its floodplain, the yolo bypass. Trans. Am. Fish. Soc. 139, 550–563.

Higson, J.L., Singer, M.B., 2015. The impact of the streamflow hydrograph on sediment supply from terrace erosion. Geomorphology 248, 475–488.

Hinkle, S., Bencala, K., Wentz, D., Krabbenhoft, D., 2014. Mercury and methylmercury dynamics in the hyporheic zone of an Oregon stream. Water Air Soil Pollut. 225, 1–17.

Hudson-Edwards, K.A., 2003. Sources, mineralogy, chemistry and fate of heavy metal-bearing particles in mining-affected river systems. Mineral. Mag. 67, 205–217.

Hunerlach, M.P., Rytuba, J.J., Alpers, C.N., 1999. Mercury contamination from hydraulic placer-gold mining in the Dutch Flat mining district, California. US Geological Survey Water-Resources Investigation Report 99-4018B, pp. 179–189.

Hurley, J.P., Cowell, S.E., Shafer, M.M., Hughes, P.E., 1998. Partitioning and transport of total and methyl mercury in the Lower Fox River, Wisconsin. Environ. Sci. Technol. 32, 1424–1432.

James, L.A., Singer, M.B., 2008. Development of the lower Sacramento Valley flood-control system: an historical perspective. Nat. Hazards Rev. 9, 125–135.

James, L.A., Singer, M.B., Ghoshal, S., Megison, M., 2009. Historical channel changes in the lower Yuba and Feather Rivers, California: long-term effects of contrasting river-management strategies. In: James, L.A., Rathburn, S.L., Whittecar, G.R. (Eds.), Management and Restoration of Fluvial Systems with Broad Historical Changes and Human Impacts. Geological Society of America Special Publication 451, pp. 57–81 http://dx.doi.org/10.1130/2008.2451(04).

Junk, W.J., Bayley, P.B., Sparks, R.E., 1989. The flood pulse concept. In: Doge, D.P. (Ed.), International Large River Symposium. Can. Fish. Aquatic Science Special Publ., pp. 110–127.

Kelley, R., 1998. Battling the Inland Sea. University of California Press, Berkeley, CA.

Kerin, E.J., Gilmour, C.C., Roden, E., Suzuki, M.T., Coates, J.D., Mason, R.P., 2006. Mercury methylation by dissimilatory iron-reducing bacteria. Appl. Environ. Microbiol. 72, 7919–7921.

Kilham, N.E., 2009. Floodplain sedimentation on the Feather River, California: combined use of remote sensing and numerical modeling to analyze contemporary deposition patterns in a historically mined basin (Department of Geography. PhD) University of California Santa Barbara, Santa Barbara, CA.

Kilham, N.E., Roberts, D., Singer, M.B., 2012. Remote sensing of suspended sediment concentration during turbid flood conditions on the Feather River. California — a modeling approach. Water Resour. Res. 48, W01521.

Krabbenhoft, D., Benoit, J., Babiarz, C., Hurley, J., Andren, A., 1995. Mercury cycling in the Allequash Creek watershed, northern Wisconsin. Water Air Soil Pollut. 80, 425–433.

Lindqvist O, Johansson K, Aastrup M, Andersson A, Bringmark L, Hovsenius G, et al. Mercury in the Swedish environment — recent research on causes, consequences and corrective methods. Water Air Soil Pollut. 1991; 55: R11-&.

Marvin-DiPasquale, M., Agee, J., 2003. Microbial mercury cycling in sediments of the San Francisco Bay-Delta. Estuaries 26, 1517–1528.

Marvin-DiPasquale, M., Agee, J.L., Kakouros, E., Kieu, L.H., Fleck, J.A., Alpers, C.N., 2011. The effects of sediment and mercury mobilization in the South Yuba River and Humbug Creek confluence area, Nevada County, California: concentrations, speciation and environmental fate — part 2: Laboratory Experiments. U.S. Geological Survey, Open-File Report 2010–1325B.

Marvin-DiPasquale, M., Alpers, C.N., Fleck, J.A., 2009a. Mercury, methylmercury, and other constituents in sediment and Water from seasonal and permanent wetlands in the Cache Creek Settling Basin and yolo bypass, Yolo County, California, 2005–06. US Geological Survey Open File Report 2009-1182, p. 69.

Marvin-DiPasquale, M., Cox, M.H., 2007. Legacy mercury in Alviso Slough, South San Francisco Bay, California: concentration, speciation and mobility. US Geological Survey Open-File Report 2007-1240, p. 98.

Marvin-DiPasquale, M., Lutz, M.A., Brigham, M.E., Krabbenhoft, D.P., Aiken, G.R., Orem, W.H., et al., 2009b. Mercury cycling in stream ecosystems. 2. Benthic methylmercury production and bed sediment–pore water partitioning. Environ. Sci. Technol. 43, 2726–2732.

Marvin-DiPasquale, M., Windham-Myers, L., Agee, J.L., Kakouros, E., Kieu, L.H., Fleck, J.A., et al., 2014. Methylmercury production in sediment from agricultural and non-agricultural wetlands in the Yolo Bypass, California, USA. Sci. Total Environ. 484, 288–299.

Marvin-DiPasquale, M.C., Oremland, R.S., 1998. Bacterial methylmercury degradation in Florida Everglades peat sediment. Environ. Sci. Technol. 32, 2556–2563.

Mason, R.P., Lawson, N.M., Lawrence, A.L., Leaner, J.J., Lee, J.G., Sheu, G.R., 1999. Mercury in the Chesapeake Bay. Mar. Chem. 65, 77–96.

McClain, M.E., Boyer, E.W., Dent, C.L., Gergel, S.E., Grimm, N.B., Groffman, P.M., et al., 2003. Biogeochemical hot spots and hot moments at the Interface of terrestrial and aquatic ecosystems. Ecosystems 6, 301–312.

Meixner, T., Manning, A.H., Stonestrom, D.A., Allen, D.M., Ajami, H., Blasch, K.W., Brookfield, A.E., Castro, C.L., Clark, J.F., Gochis, D.J., Flint, A.L., Neff, K.L., Niraula, R.,

Rodell, M., Scanlon, B.R., Singha, K., Walvoord, M.A., 2016. Implications of projected climate change for groundwater recharge in the western United States. J. Hydrol. 534, 124–138.

Mergler, D., Anderson, H.A., Chan, L.H.M., Mahaffey, K.R., Murray, M., Sakamoto, M., et al., 2007. Methylmercury exposure and health effects in humans: a worldwide concern. AMBIO: A Journal of the Human Environment 36, 3–11.

Miller, J., Barr, R., Grow, D., Lechler, P., Richardson, D., Waltman, K., et al., 1999. Effects of the 1997 flood on the transport and storage of sediment and mercury within the Carson River valley, west-central Nevada. J. Geol. 107, 313–327.

Miller, J.R., 1997. The role of fluvial geomorphic processes in the dispersal of heavy metals from mine sites. J. Geochem. Explor. 58, 101–118.

Moir, H.J., Pasternack, G.B., 2010. Substrate requirements of spawning Chinook salmon (*Oncorhynchus tshawytscha*) are dependent on local channel hydraulics. River Res. Appl. 26, 456–468.

Pasternack, G.B., Morford, S.L., Fulton, A.A., 2010. Yuba River analysis aims to aid spring-run chinook salmon habitat rehabilitation. Calif. Agric. 64, 69–77.

Pizzuto, J., 2012. Predicting the accumulation of mercury-contaminated sediment on riverbanks: An analytical approach. Water Resour. Res. 48, W07518.

Podar, M., Gilmour, C.C., Brandt, C.C., Soren, A., Brown, S.D., Crable, B.R., et al., 2015. Global prevalence and distribution of genes and microorganisms involved in mercury methylation. Sci. Adv. 1.

Schaefer, J.K., Morel, F.M.M., 2009. High methylation rates of mercury bound to cysteine by *Geobacter sulfurreducens*. Nat. Geosci. 2, 123–126.

Singer, M.B., 2007. The influence of major dams on hydrology through the drainage network of the Sacramento Valley, California. River Res. Appl. 23, 55–72.

Singer, M.B., 2008a. Downstream patterns of bed-material grain size in a large, lowland alluvial river subject to low sediment supply. Water Resour. Res. 44, W12202. http://dx.doi.org/10.1029/2008WR007183.

Singer, M.B., 2008b. A new sampler for extracting bed material sediment from sand and gravel beds in navigable rivers. Earth Surf. Process. Landf. 33, 2277–2284.

Singer, M.B., 2010. Transient response in longitudinal grain size to reduced gravel supply in a large river. Geophys. Res. Lett. 37, L18403. http://dx.doi.org/10.1029/2010gl044381.

Singer, M.B., Aalto, R., James, L.A., 2008. Status of the lower Sacramento Valley flood-control system within the context of its natural geomorphic setting. Nat. Hazards Rev. 9, 104–115.

Singer, M.B., Aalto, R., James, L.A., Kilham, N.E., Higson, J.L., Ghoshal, S., 2013. Enduring legacy of a toxic fan via episodic redistribution of California gold mining debris. Proc. Natl. Acad. Sci. 110, 18436–18441.

Sommer, T., Harrell, B., Nobriga, M., Brown, R., Moyle, P., Kimmerer, W., et al., 2001. California's Yolo Bypass: evidence that flood control can be compatible with fisheries, wetlands, wildlife, and agriculture. Fisheries 26, 6–16.

Sorensen, J.A., Kallemeyn, L.W., Sydor, M., 2005. Relationship between mercury accumulation in young-of-the-year yellow perch and water-level fluctuations. Environ. Sci. Technol. 39, 9237–9243.

Springborn, M., Singer, M.B., Dunne, T., 2011. Sediment-adsorbed total mercury flux through Yolo Bypass, the primary floodway and wetland in the Sacramento Valley, California. Sci. Total Environ. 412-413, 203–213.

St. Louis VL, Rudd, JWM, Kelly, CA, Beaty, KG, Bloom, NS, Flett, RJImportance of wetlands as sources of methyl mercury to boreal forest ecosystems. Can. J. Fish Aquat. Sci. 1994; 51: 1065-1076.

Stonestreet, S.E., Lee, A.S., 2000. Use of LIDAR Mapping for Floodplain Studies. Building Partnerships-2000 Joint Conference on Water Resource Engineering, Planning, and Management. US Army Corps of Engineers, Sacramento, Ca.

Suchanek, T.H., Mullen, L.H., Lamphere, B.A., Richerson, P.J., Woodmansee, C.E., Slotton, D.G., et al., 1998. Redistribution of mercury from contaminated lake sediments of Clear Lake, California. Water Air Soil Pollut. 104, 77–102.

Tockner, K., Malard, F., Ward, J.V., 2000. An extension of the flood pulse concept. Hydrol. Process. 14, 2861–2883.

Trigg, M.A., Michaelides, K., Neal, J.C., Bates, P.D., 2013. Surface water connectivity dynamics of a large scale extreme flood. J. Hydrol. 505, 138–149.

Tsui MT, Finlay JC, Nollet YH, Balogh SJ. In-stream production of methylmercury in a northern California river during summer baseflow. American Geophysical Union Fall Meeting. 90(52), (Fall Meet. Suppl., Abstract H54C-06). AGU, San Francisco, 2009a.

Tsui, M.T.K., Finlay, J.C., Nater, E.A., 2009b. Mercury bioaccumulation in a stream network. Environ. Sci. Technol. 43, 7016–7022.

Ullrich, S.M., Llyushchenko, M.A., Uskov, G.A., Tanton, T.W., 2007. Mercury distribution and transport in a contaminated river system in Kazakhstan and associated impacts on aquatic biota. Appl. Geochem. 22, 2706–2734.

van Geen, A., Luoma, S.N., 1999. The impact of human activities on sediments of San Francisco Bay, California: an overview. Marine Chem. 64, 1–6.

Vroblesky, D.A., Chapelle, F.H., 1994. Temporal and spatial changes in terminal electron-accepting processes in a petroleum hydrocarbon-contaminated aquifer and the significance for contaminant biodegradation. Water Resour. Res. 30, 1561–1570.

Wallschlager, D., Desai, M.V.M., Spengler, M., Windmoller, C.C., Wilken, R.D., 1998. How humic substances dominate mercury geochemistry in contaminated floodplain soils and sediments. J. Environ. Qual. 27, 1044–1054.

Zarnetske JP, Haggerty R, Wondzell SM, Baker MA. Dynamics of nitrate production and removal as a function of residence time in the hyporheic zone. Journal of Geophysical Research: Biogeosciences 2011; 116: n/a-n/a.